

THE $\bar{p}p$ PROGRAM AT FERMILAB

P.M. McIntyre
Fermi National Accelerator Laboratory*
Batavia, Illinois 60510

Abstract

The \bar{p} source and $\bar{p}p$ scenario at Fermilab are described. The \bar{p} source can accumulate $N_{-} = 10^{10}/\text{hr}$. Proton-antiproton collisions at $\sqrt{s} = 2 \text{ TeV}$ in the Energy Doubler have a luminosity of $\mathcal{L} = 2 \times 10^{29} \text{ cm}^{-2} \text{ sec}^{-1}$. A novel use for the \bar{p} source is to study \bar{p} -heavy nucleus collisions using an internal target with a 1 TeV p beam in the Energy Doubler. It is possible in this way to produce new particles in the mass range $30\text{--}60 \text{ GeV}/c^2$, and to study direct photon and lepton production for large p_T .

It was suggested in 1976¹⁾ that the present high energy synchrotrons at CERN and Fermilab could be operated as $\bar{p}p$ storage rings with a center-of-mass energy of some 800 GeV. The Fermilab Energy Doubler/Saver, in addition, could be quite suitable as a high performance storage ring, producing collisions at 2 TeV in the center-of-mass. Both laboratories have subsequently decided to develop an antiproton source and $\bar{p}p$ colliding beams program.^{2,3)} Design and construction of experiments is underway at both laboratories for large $\bar{p}p$ colliding beam experiments.⁴⁾ In this paper, I will describe the \bar{p} source and the scenario for achieving a $\bar{p}p$ colliding beams program at Fermilab. I will also describe a possible experiment to observe high energy \bar{p} interactions with a heavy nucleus internal target.

I. THE $\bar{p}p$ PROGRAM AT FERMILAB

The \bar{p} Source

In order to achieve useful luminosity in $\bar{p}p$ collisions, it is necessary to: 1) collect antiprotons from ~80 GeV protons colliding on a stationary target, 2) cool the phase space of the initially diffuse \bar{p} 's, and 3) accumulate the cooled \bar{p} 's over many cycles. Several methods have been devised to carry out this repetitive accumulation and cooling.^{5,6)} The method used at Fermilab is that of electron cooling. The "hot" antiprotons are injected into a storage ring and brought into conjunction with an intense "cold" electron beam in one straight section. If the electrons and antiprotons have the same mean vector velocity, the two beams will interact via Coulomb collisions in the rest frame, and the \bar{p} 's will transfer their heat content to the electrons. If the initial relative velocities in the rest frame are modest, this heat transfer can be quite rapid.

Electron cooling was first demonstrated by G. I. Budker et al.⁷⁾ They have efficiently damped both the betatron motion and momentum spread of a beam of 65 MeV protons in approximately 80 milliseconds.

In order to adapt this technique to antiproton cooling, one faces the problem that phase space compression with

electrons works efficiently only at non-relativistic energies, while the greatest majority of \bar{p} 's are produced fast in the laboratory system, i.e., $\langle \gamma \rangle_p \sim \sqrt{E_p/2m} = 7$. The region between the optimum production and cooling energies for antiprotons may be covered by the introduction of a deceleration stage between the production of \bar{p} 's and the subsequent electron cooling.²⁾ A design has been developed to use the rapid-cycling Fermilab booster to decelerate \bar{p} 's to 200 MeV where electron cooling and stacking could be performed in a modest cooling ring.

The \bar{p} accumulation is described in Ref. 2, and is shown schematically in Fig. 1. Antiprotons at 6 GeV ($x=0$) are produced on a small tungsten target by 80 GeV protons. They are injected into the booster accelerator and decelerated to 200 MeV. They are transferred to the electron cooling ring. An electron cooling time of 50 msec allows this beam to be cooled and stacked while the (15 Hz) booster ramps back to 6 GeV and takes a fresh production cycle from the main ring. In this way the entire contents of the main ring are targeted in 13 booster-length segments to make and accumulate antiprotons.

The phase space acceptance of this \bar{p} source is limited by 1) the low-energy acceptance of the booster: $p_{\perp} \sim 70$ MeV/c $\delta p_{\perp} \sim 15$ MeV/c; 2) the strong dependence ($\propto p_{\perp}^3$) of the cooling time on initial \bar{p} temperature. The initial \bar{p} production is accommodated to the acceptance of the booster by 1) making a very strong focus ($\beta^* = 2$ cm) at the production target, and 2) moving the transition energy of the booster to optimally capture the tight bunch structure of the antiprotons.²⁾

The above scenario results in accumulation of $\sim 1 \times 10^7$ \bar{p} 's in each main ring cycle of 3 seconds, corresponding to $\dot{N}_{\bar{p}} \sim 1 \times 10^{10}/\text{hr.}$

A major improvement to this scenario is presently being designed. The hot antiprotons would first be stored in a large-aperture storage ring at production energy (6 GeV), and there be pre-cooled in momentum spread by a factor ~ 7 using stochastic cooling.⁸⁾ The \bar{p} 's would then be extracted by RF peeling, decelerated in the booster and accumulated in the electron cooling ring. By peeling and accumulating ~ 25 booster-acceptance

beams from the pre-cooled stock, the average accumulation rate is enhanced by a factor ~7-10.

pp Colliding Beams

With this \bar{p} source (sans pre-cooler), $N_{\bar{p}} \sim 3 \times 10^{10}$ can be accumulated in 3 hours time. The antiprotons are then bunched into ~7 RF buckets in the electron cooling ring, and transferred one at a time through the booster and main ring to the Energy Doubler/Saver. High intensity ($n_{\bar{p}} \sim 10^{11}$ /bunch) proton bunches are prepared in the main ring by RF rebunching, and then transferred to the Energy Doubler counter-rotating to the \bar{p} 's. At the interaction points where experiments will be located, a low β insertion has been designed⁹⁾ with $\beta^* = 1.5$ m and $\eta = \eta' = 0$. This corresponds to a luminosity of $\mathcal{L} \approx 2 \times 10^{29} \text{ cm}^{-2} \text{ sec}^{-1}$. When the pre-cooler ring is added to the \bar{p} source, this luminosity would increase by one order of magnitude.

II. COLLIDING 1 TEV "ANTIQUARKS" ON HEAVY NUCLEI

The physics merits of $\bar{p}p$ experiments are well-known. The valence antiquark structure of the antiproton permits a completely new exploration of high energy phenomena: 1) enhanced production near threshold of high-mass states; 2) a distinct channel for the study of deep hadronic processes, e.g., continuum di-leptons and photons. These definite advantages are, however, usually lost due to the drastic reductions in energy as well as intensity of secondary antiproton beams. Francis Halzen and I have investigated the possibility of eliminating the experimental handicaps by using the antiproton source in conjunction with heavy nuclear internal targets.¹⁰⁾

In the experiments of Dorfan et al.,¹¹⁾ antiprotons were produced by colliding a 3 GeV proton beam with a Cu-target, although 5.6 GeV is required for the reaction $pp \rightarrow p\bar{p}pp$. The extra energy is supplied by the Fermi momentum q of the nucleons inside the target nucleus, contributing approximately an amount ($2 p_0 q$) to the center of mass energy squared s available in the collision:

$$s(\vec{q}) = 2m^2 + 2E_0(q^2 + m^2)^{1/2} - 2\vec{p}_0 \cdot \vec{q} \quad (1)$$

The \bar{p} -experiments at Berkeley actually demonstrated that Fermi momenta up to 0.65 GeV/c are available in heavy nuclei (see Fig. 2). With an incident momentum $p_0 = 1000$ GeV/c this Fermi momentum corresponds to $s = 3600$ GeV 2 --highest energy available with the CERN ISR. On purely kinematic grounds one would therefore conclude that with the Fermilab Energy Doubler it is possible to produce masses as large as 60 GeV/c 2 .

The mass range (30-60) GeV/c 2 is very tantalizing for physics. The charged weak intermediate boson W^+ could be as light as 55 GeV/c 2 in conventional¹²⁾ (and lighter in unconventional¹³⁾) models which unify the weak and electromagnetic interactions. The t-quark is expected¹⁴⁾ to have a mass $\sim 15-30$ GeV/c 2 , possibly putting it out of reach of the new generation e^+e^- machines, but within the reach of Fermilab's Energy Doubler.

New Particle Production Cross-Sections

Despite recent studies of Ψ and T production, little is known about the dynamics of new particle production very near threshold. According to quantum chromodynamics, the production of heavy flavor bound states and pairs of new quarks near threshold proceeds via fusion of a quark and antiquark,¹⁵⁾ and gluon-induced production mechanisms are negligible. The cross-section can be calculated using the measured structure functions of the hadrons. Because of the moderate range of extrapolation in \sqrt{s} and M , scaling violations can be neglected. However, as in the present discussion we consider particle production near the kinematic limit, phase space considerations must play an important role.

We have calculated the production cross-section according to two models:

- 1) the Drell-Yan mechanism: $q + \bar{q} \rightarrow \gamma^* \rightarrow X$;
- 2) a phase space calculation which is normalized to the Drell-Yan cross-section far above threshold.

1) Drell-Yan mechanism

The production cross section at Feynman $x_F = 0$ is given by

$$\sigma \equiv x_0 \frac{d\sigma}{dx_F} = g^2 \frac{1}{3} x^2 \bar{q}(x) q(x) \quad (2)$$

Summation over allowed types of quarks is understood, and $q(x)$

and $\bar{q}(x)$ describe the fractional momentum (x) distributions of quarks and antiquarks inside the initial hadrons.

The crucial observation is that $\sigma \sim u(x) s(x)$ in the case of pp collisions while $\sigma \sim u^2(x)$ for $\bar{p}p$ or πp collisions; $u(x)$ and $s(x)$ are the x distributions for valence and sea quarks, respectively. Typically¹⁵⁾

$$\begin{aligned} u_p(x) &= 1.79 (1 + 2.3x) (1 - x)^3 / \sqrt{x} \\ u_{\pi}(x) &= 0.75 (1 - x) / \sqrt{x} \\ s(x) &= 0.44 (1 - x)^{10} / x \end{aligned} \quad (3)$$

The production cross-sections in pp , $\bar{p}p$, and πp collisions are then

$$\begin{aligned} \sigma_{pp} &\propto (1 - x)^{13} \\ \sigma_{\bar{p}p} &\propto (1 - x)^6 \\ \sigma_{\pi p} &\propto (1 - x)^4 \end{aligned}$$

where $(1 - x)$ is the Q -value of the production process. Because we are considering particle production near threshold, there is a strong enhancement ($\gtrsim Q^7$) by using valence rather than sea quarks. Note that this enormous advantage is not enjoyed in comparing $\bar{p}p$ vs pp colliding beams, where processes of interest generally require only modest x .

The calculation of the nuclear cross sections is straightforward; the procedure is described in detail in Refs. 16,17. We start by unfolding the \bar{p} -data to deduce an effective momentum distribution of nucleons inside heavy nuclei. Since the nuclear wave functions do not reliably determine the large q tail of the momentum distribution, we use this effective momentum distribution deduced with on-shell kinematics.¹¹⁾ As is well-known,¹¹⁾ this leads to a power-law q^2 distribution of the Hulthén type whose parameters are determined by the \bar{p} -data. This phenomenological distribution is subsequently used to calculate the cross-section for producing a new particle of mass M on a U target. We assume an explicit nuclear dependence $\sigma \propto A^{1.0}$.¹⁸⁾

Table I shows the resulting cross sections for the production of the topsilon $T(t\bar{t})$ —the bound state of the charge

2/3 partner of the b-quark--assuming representative mass values $M = 30, 56$ GeV. Production by \bar{p} and π beams is enhanced a factor $\gtrsim 10^5$ relative to production by protons.

2) Phase space calculation

For each particle in the final state, the available phase space $\frac{d^3p}{E}$ contributes a factor $Q^{3/2}$ to the differential cross-section; after integration¹⁹⁾ one obtains

$$\sigma \propto Q^{[3n-5]/2} \quad (4)$$

where n is the number of particles in the final state. Charge and baryon number conservation require that at least 2 particles accompany a heavy vector meson produced in a proton or pion induced interaction (e.g., $pp \rightarrow pp\pi^-$), yielding $n \geq 3$. These constraints are less stringent in \bar{p} interactions, where $n \geq 2$. We have calculated production cross sections assuming the behavior of Eq. 4 at all x , with normalization to the Drell-Yan cross-section (Eq. 1) when $x \rightarrow 0$. The results are shown in Table I.

In order to illustrate the relevance of the phase space calculation, we applied it to the \bar{p} production data ($Q^{3.5}$) of Dorfan et al.,¹¹⁾ after normalizing the input pp cross-section at energies far above threshold. The agreement is impressive (see Fig. 1).

Figure 3 exhibits the mass dependence of the cross-section per nucleus for \bar{p} uranium interactions using alternatively the Drell-Yan and phase space calculations. The phase space calculation represents the maximum cross section one can expect using Fermi motion, whereas the Drell-Yan model almost certainly underestimates the nuclear effects and threshold behavior. The leptonic branching fraction is not sensitive to the mass and has been assumed²⁰⁾ to be 10%.

QCD Predictions for Continuum Dileptons and Photons

High energy antiproton collisions provide an attractive channel for studying direct production of leptons and photons. The event rates and backgrounds permit detection of electrons, muons, and photons in the final state, with large acceptance for modest x_F . This capability is valuable for observing several processes of current interest in QCD, as described below.

In an interaction where a pair of new quarks (e.g., t, \bar{t}) are produced, an $e\bar{e}$ final state constitutes the most distinct signature for identifying associated production of a naked new flavor:

$$\begin{aligned}\bar{p}N &\rightarrow t \bar{t} X \\ &\quad b \bar{e}^- \bar{\nu}_e \\ &\quad b \mu^+ \nu_\mu\end{aligned}$$

The leptons should have sufficient p_\perp ($\sim M/3$) to distinguish them from low-mass and continuum sources. Indeed, naked flavor production and decay may be more easily identified than the di-lepton decays from hidden flavor vector mesons ($T = t\bar{t}$), where continuum background could obscure resonance structure for large mass states.²⁰⁾

For single lepton and photon production, there are now specific QCD predictions:¹⁵⁾ 1) \bar{p}/p ratios as a function of p_\perp ; 2) γ/π ratio should increase dramatically for $p_\perp > 6$ GeV/c, with an associated increase in ℓ/π through internal conversion.

Cross-sections for continuum dilepton production²⁰⁾ are at least as large as those for the Topsilon. It should thus be possible to observe continuum production in the range 30-60 GeV/c². This permits an extended test of scaling in $\bar{p}p$ interactions, and measurement of A dependence in deep inelastic processes.

\bar{p} -heavy Nucleus Collisions

The \bar{p} source is expected to be operating when the Energy Doubler first circulates beam. It will then be possible to inject antiprotons into the Energy Doubler, circulating in the reverse direction to normal proton operation. Since they are traveling opposite to the usual proton orbits, extraction to the existing beam lines is precluded.²¹⁾ A fixed target experiment can thus only be done by injecting a heavy nuclear target into the beam inside the Energy Doubler. This technique has been used successfully on the Main Ring at the Internal Target Facility. Two possibilities suggest themselves: 1) a rotating wire target, in which $\sim 2\mu\text{m}$ wires of W_{184} or U_{238} are spinning rapidly through the beam; and 2) a Hg_{200} vapor jet, in which

an $\sim 0.1 - 1$ Torr jet of mercury vapor passes through the beam and is then condensed on baffle plates.

The utility of these techniques depends upon the balance between nuclear collisions and beam growth due to multiple scattering from the electrons of the target. The nuclear collision rate is $\Gamma = L \sigma_n$, where L is the luminosity for nuclear interactions, and $\sigma_n \approx \sigma_{tot} A^{2/3}$ is the total cross-section per nucleus.

$$L = f N_p n \lambda, \quad (5)$$

where $f = 4.7 \times 10^4 \text{ sec}^{-1}$ is the revolution frequency,

$n_p [\text{cm}^{-3}]$ = number density of heavy nuclei,

$\lambda [\text{cm}]$ = target length.

For $A = 200$, $\sigma_{tot} \sim 40 \text{ mb}$, this corresponds to

$$\Gamma = 6 \times 10^{-20} N_p n \lambda. \quad (6)$$

Guignard²²⁾ has calculated the rate of beam growth due to multiple small-angle Coulomb scattering:

$$\frac{1}{T} = \frac{1}{\sigma} \frac{d\sigma}{dt} = k \frac{\beta^* n_p z^2}{p \epsilon_0} \frac{\lambda}{2\pi R}$$

where $\beta^* [\text{m}]$ = local betatron function of the storage ring lattice,

$p = 1000 \text{ GeV}$ is the \bar{p} beam momentum,
 $\epsilon_0 \approx 20\pi 10^{-6} \text{ m}$ is the (invariant) initial beam emittance,

$R = 10^5 \text{ cm}$ is the ring radius,
 $k = 1.8 \times 10^{-19} \text{ cm}^3 \text{ GeV sec}^{-1}$.

For $z = 80$, this corresponds to

$$\frac{1}{T} = 3 \times 10^{-20} \beta^* n_p \lambda. \quad (7)$$

The "efficiency" of targeting antiprotons is thus the fraction $\epsilon = \Gamma / (T + N_p / T) = 1 / (1 + \beta^* / \beta_0)$, where $\beta_0 = 2 \text{ m}$. A local $\beta^* \sim 1.5 \text{ m}$ is already envisioned in at least one long straight section in the Energy Doubler, to accommodate $\bar{p}p$ colliding beams.⁹⁾ This corresponds to $\epsilon \sim 1/2$: roughly half of all

\bar{p} 's actually produce nuclear collisions in the target.

The useful luminosity is thus

$$L = \epsilon \dot{N}_p^- / \sigma_n = 8 \times 10^{29} \text{ cm}^{-2} \text{ sec}^{-1}$$

One event per hour would correspond to a cross-section \times branching fraction $\sigma \cdot B = 3 \times 10^{-34} \text{ cm}^2/\text{nucleus}$.

Consequences for Experiments

We have similarly calculated new particle production by protons and pions, assuming the highest intensity p , π^+ beams contemplated for the Energy Doubler.¹⁰⁾ These calculations span the range of expectations (neglecting coherent effects) for new particle production near threshold. To illustrate the consequences for prospective experiments we consider two cases from Table I.

1) Drell-Yan mechanism: production of a new vector meson with mass $M_T = 30 \text{ GeV}/c^2$, branching fraction $B = 0.1$:

$$\begin{aligned} 1000 \text{ GeV } \bar{p} + U - & 30 \\ 900 \text{ GeV } \pi^+ + U - & 480 \text{ events/hour} \\ 1000 \text{ GeV } p + U - & 1280 \end{aligned} \quad (8)$$

2) Phase space calculation: production of a new vector meson with mass $M_T = 56 \text{ GeV}/c^2$, branching fraction $B = 0.1$:

$$\begin{aligned} 1000 \text{ GeV } \bar{p} + U - & 2 \\ 900 \text{ GeV } \pi^+ + U - & 4 \times 10^{-4} \text{ events/hour} \\ 1000 \text{ GeV } p + U - & 0.7 \end{aligned} \quad (9)$$

It is thus possible to produce new particles in the mass range $(30-60) \text{ GeV}/c^2$, depending on which production mechanism prevails near threshold. To compare possible experiments using \bar{p} , π^+ , and p beams, it is essential to examine the backgrounds present for di-lepton decay signatures. In this respect \bar{p} and π^+ beams exhibit an enormous advantage over p beams: the production cross-section is greater by a factor $\sim 10^3 - 10^5$, while one expects background cross-sections to be comparable. This advantage can be useful in two ways. First, the signal/background improvement further extends the useful mass range. Second, the much smaller total interaction rate (\dot{N}_p^- , \dot{N}_{π^+} + $\langle \dot{N}_p \rangle$) should be compatible with experiments to detect $e^+ e^-$ decays,

as well as the $\mu^+ \mu^-$ decays sought in high-rate proton experiments. By detecting $e^+ e^-$ final states, a $\bar{p}N$ experiment could achieve a mass resolution $\sim 0.3\%$ for new vector mesons.¹⁰⁾ Furthermore, \bar{p} interactions occur continuously during an internal target experiment, while π^+ and p beams for the Energy Doubler will have a time duty factor $\sim 2\%$.

If a vector meson is produced at $x_F = 0$, $p_\perp = 0$, and decays into two leptons, the leptons emerge in the lab frame in an angular distribution peaked at $\theta_o = 1/\beta \gamma^* = \sqrt{s}/p_o \approx 43$ mrad for the Energy Doubler.²³⁾ Leptons from weak decays of naked flavor states also peak at θ_o , although the distribution is broader. Direct photons produced at $x_F = 0$, $p_\perp = 0$ also emerge at θ_o . The geometry of an internal target experiment permits large acceptance in the angular region $10 < \theta < 100$ mrad, so that all the above-mentioned physics could be studied in the same detector.

References

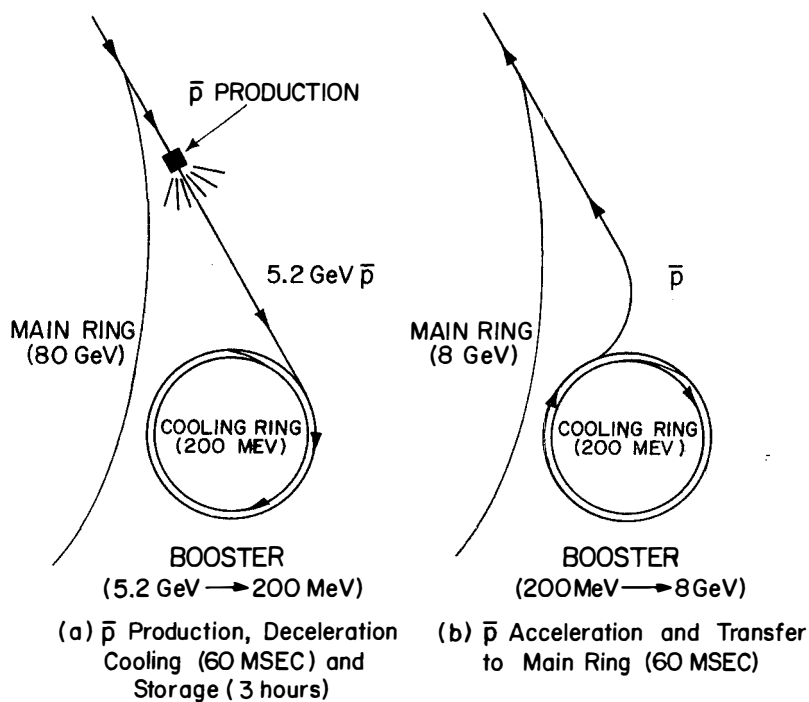
*Operated by Universities Research Association, Inc. under contract with the United States Department of Energy.

- 1) C. Rubbia, P. McIntyre and D. Cline, "Producing Massive Intermediate Vector Meson with Existing Accelerators", submitted to Phys. Rev. Letters, March 1976. Rejected!
- 2) D. Cline, P. McIntyre, F. Mills and C. Rubbia, "Collecting Antiprotons in the Fermilab Booster and Very High Energy pp Collisions", Fermilab TM-689, August 1976. "Fermilab Electron Cooling Experiment", Design Report, Fermi National Accelerator Laboratory, Batavia, IL, August, 1978.
- 3) CERN AA Design Report.
- 4) J. Dowell, this volume; and C. Ankenbrandt et al., "Design of a Magnetic Detector Facility for Colliding Beams at Fermilab", 1979.
- 5) G. I. Budker, Atomic Energy 22, 346 (1967); G. I. Budker, et al., "Experimental Facility for Electron Cooling", BNL-TU-588 (1974); "Preliminary Experiments on Electron Cooling", BNL-TR-593 (1974); "Experimental Study of Electron Cooling", BNL-TR-635 (1976).
- 6) S. Van der Meer, CERN-ISR-PS/72-31, August, 1972 (unpublished).
- 7) G. I. Budker, et al., "New Results of Electron Cooling Studies", Nat. USSR Conf. on High Energy Accelerators (Dubna) Oct. 2, 1976.
- 8) S. Van der Meer, "Pre-cooling in the Antiproton Accumulator", CERN/PS/AA/78-26, 12 December 1978.

- 9) D. Johnson, "High Luminosity pp and $\bar{p}p$ Colliding Beam Straight Section Designs, Fermilab TM-876, April 13, 1979.
- 10) F. Halzen and P. McIntyre, "Very High Energy Antiproton Physics: Colliding 1 TeV 'Antiquarks' with Heavy Nuclei", submitted to Phys. Rev., May, 1979.
- 11) D. E. Dorfan et al., Phys. Rev. Lett. 14, 995 (1965); P. A. Piroué et al., Phys. Rev. 148, 1315 (1966).
- 12) J. D. Bjorken, SLAC-PUB-1841 (1976).
- 13) See e.g., R. N. Mohapatra and J. C. Pati, Phys. Rev. D11, 566 (1975).
- 14) The usual argument is $m_c/m_s \approx m_t/m_b \approx 3$. The higher values have been argued for by J. D. Bjorken, SLAC-PUB 2195 (1978); S. Pakvasa and H. Sugawara, University of Wisconsin, COO-881-66 (1978).
- 15) For recent reviews see, e.g., R. Field, F. Halzen and L. Lederman in Proc. XIX International Conf. on High Energy Physics, Tokyo, Japan (1978).
- 16) T. K. Gaisser, F. Halzen and E. A. Paschos, Phys. Rev. D15, 2572 (1977).
- 17) T. K. Gaisser and F. Halzen, Phys. Rev. D11, 3157 (1975).
- 18) See, e.g., L. Lederman and B. Pope, Phys. Lett. 66B, 486 (1977).
- 19) See, e.g., R. Hagedorn, Relativistic Kinematics, (Benjamin, Redding, Mass., 1973).
- 20) F. Halzen, University of Wisconsin, COO-881-71, to be published in the Proc. Topical Conf. on Cosmic Rays and Particle Physics above 10 TeV, Bartol Research Foundation at the University of Delaware (1978), F. Halzen and S. Pakvasa, in preparation.
- 21) To circulate \bar{p} 's in the same sense as protons would require reversing both Main Ring and Energy Doubler power supplies; that is a costly modification, and we do not consider it here.
- 22) G. Guignard, Selection of Formulae Concerning Proton Storage Rings, CERN 77-10 (1977).
- 23) S. C. C. Ting, Proceedings from 1975 International Symposium on Lepton and Photon Interactions at High Energies, Stanford University, Stanford, Calif., August 21-27, 1975, pp. 155-188.

Figure Captions

1. \bar{p} Source at Fermilab.
2. \bar{p} production below threshold. Data are from Ref. 11. The curve represents the phase space calculation for $pp \rightarrow pppp$.
3. Cross-section for producing a new vector meson using $p_T = 1$ TeV. Estimates are shown for a) pp (Drell-Yan); b) $\bar{p}p$ (Drell-Yan); c) $\bar{p}U$ (Drell-Yan); and d) $\bar{p}U$ (phase space). Cross-sections for a) and b) have been multiplied by $A = 238$ for comparison with c) and d).



\bar{p} SOURCE AT FERMILAB

Fig. 1

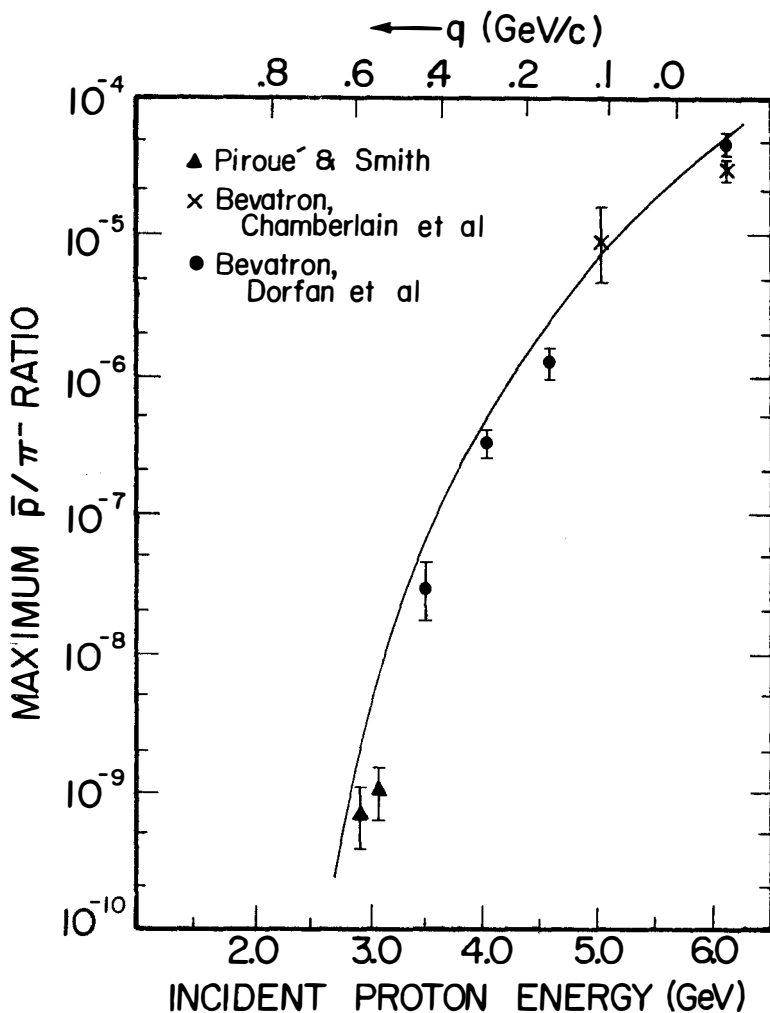


Fig. 2

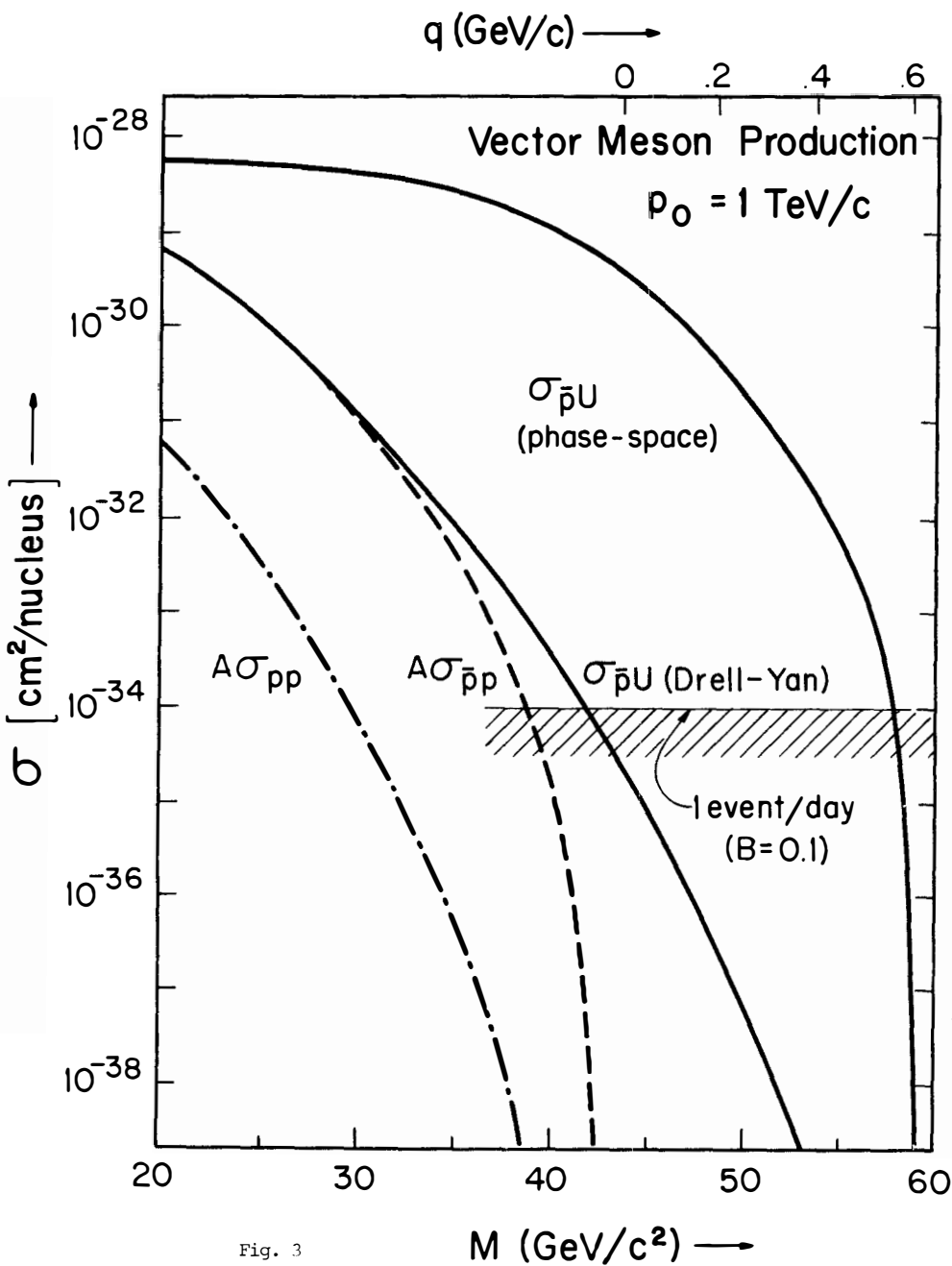


Fig. 3